# Examination of the photoinitiation processes in photopolymer materials

Michael R. Gleeson,[1,2,3,a] Shui Liu,[1,2,3] Sean O'Duill,[1,2] and John T. Sheridan[1,2,3,b]
[1]*UCD School of Electrical, Electronic and Mechanical Engineering, University College Dublin, Belfield, Dublin 4, Ireland*
[2]*Optoelectronic Research Centre, University College Dublin, Belfield, Dublin 4, Ireland*
[3]*SFI Strategic Research Centre in Solar Energy Conversion, College of Engineering, Mathematical and Physical Sciences, University College Dublin, Belfield, Dublin 4, Ireland*

(Received 11 May 2008; accepted 29 July 2008; published online 29 September 2008)

Holographic data storage requires multiple sequential short exposures. However, the complete exposure schedule may not necessarily occur over a short time interval. Therefore, knowledge of the temporally varying absorptive effects of photopolymer materials becomes an important factor. In this paper, the time varying absorptive effects of an acrylamide/polyvinylalcohol photopolymer material are examined. These effects are divided into three main photochemical processes, which following identification, are theoretically and experimentally examined. These processes are (i) photon absorption, (ii) photosensitizer recovery, and (iii) photosensitizer bleaching. © *2008 American Institute of Physics*. [DOI: 10.1063/1.2985905]

## I. INTRODUCTION

In the literature, extensive studies have been carried out on the storage capabilities of photopolymer materials due to their ability to record low loss, low shrinkage, high diffraction efficient volume holographic gratings.[1–10] These self-processing materials are inexpensive and provide storage characteristics, which make them suitable for commercial use.[9,10] Obtaining their full potential requires quantitative insight into the processes present during holographic recording. Developing accurate theoretical models, which are validated using reproducible experimental data sets, will allow crucial material parameters to be identified and controlled.

The specific focus of the work presented in this paper is the initiation mechanisms, which occur in these photopolymer materials during illumination. When a photopolymer material absorbs photons, primary (initiator) radicals, $R^{\bullet}$, are created. These free radicals can then react with monomer molecules within the material, to produce macroradicals, $M^{\bullet}$. The macroradicals can then react with monomer to form propagating polymer chains, resulting in a change in the material's density in the exposed regions, and hence a change in the refractive index. It is this recorded change in refractive index that enables a photopolymer material to store information using holographic techniques.

If it is possible to precisely measure the number of photons being absorbed by the photopolymer material, then an accurate theoretical representation of the photopolymerization process can be made. Therefore, in order to fully predict the temporal evolution of holographic grating formation, it is necessary to thoroughly examine the kinetics of photoinitiation in photopolymer materials. Thus, we aim to further develop existing theories of the photoinitiation processes,[1–14] by theoretically and experimentally examining these temporal effects during and postexposure.

This paper is organized as follows: In Sec. II, we begin by discussing the photochemical reactions, which determine the photopolymerization processes during grating formation. A flow chart is presented, which succinctly summarizes these photochemical reactions. The processes which remove (bleaching) and replenish (recovery) the active absorptive photosensitizer are also discussed, and a general rate equation for this behavior is presented. Section III is split up into three subsections: (A) presents a theoretical analysis of the photosensitizer behavior during and postexposure, (B) describes an experimental examination of the photosensitizer concentration during exposure, and (C) examines the effects of the photosensitizer recovery and photobleaching postexposure. Section IV contains a brief discussion and conclusion.

## II. PHOTOCHEMICAL ANALYSIS

### A. Initiation mechanisms

The initiation step in our photopolymer material is considered to involve two main reactions. The *first* of these reactions, shown in Eq. (1), is the production of primary radicals, $R^{\bullet}$, by homolytic dissociation of a photoinitiator or catalyst species $I$

$$I \xrightarrow{k_d} 2R^{\bullet}, \tag{1}$$

where $k_d$ is the rate constant for the catalyst dissociation and the factor of 2 indicates that radicals are created in pairs.[15] This reaction occurs when the photoinitiator species absorbs the incident photons of a suitable wavelength. In our analysis, the photoinitiator consists of a photosensitive dye (Erythrosin B) denoted by Dye, and an electron donor (ED), i.e., triethanolamine $(HOCH_2CH_2)_3N$.[16–18]

The *second* reaction in the initiation process involves the primary radicals, which are produced due to the absorption of photons, reacting with monomer molecules to produce the chain initiating or macroradical species, $M_1^{\bullet}$,[15,18–20]

[a]Electronic mail: mgleeson@ee.ucd.ie.
[b]Author to whom correspondence should be addressed. Electronic mail: john.sheridan@ucd.ie. Tel.: +353-1-716-1927. FAX: +353-1-283-0921.

 

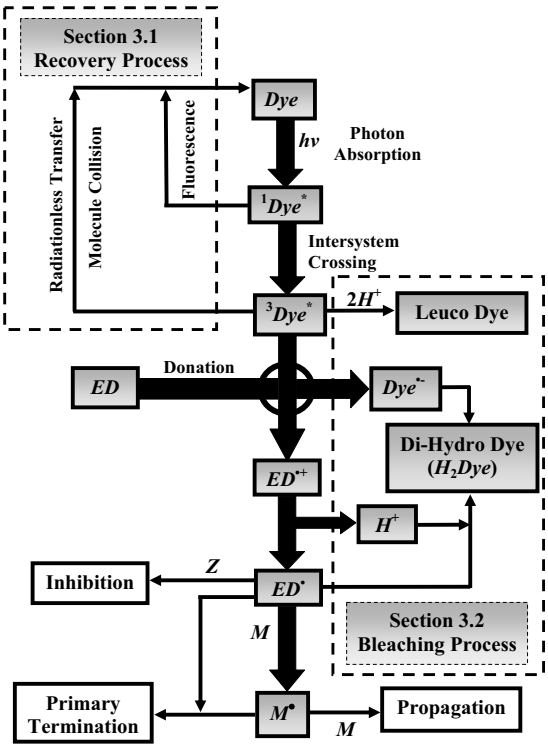


FIG. 1. Flow chart of the photoinitiation mechanisms present in our photopolymer material.

$$R^\bullet + M \xrightarrow{k_i} M_1^\bullet, \tag{2}$$

where $k_i$ is the initiation rate constant associated with this reaction. The macroradical, $M_1^\bullet$, then propagates by bonding with other monomer molecules to form polymer chains.

In the first initiation reaction, when the photosensitizer is exposed to light of a suitable wavelength, it absorbs photons and is promoted into a singlet excited state, $^1Dye^*$,[21]

$$Dye + h\nu(photons) \rightarrow {}^1Dye^*. \tag{3}$$

The singlet excited state dye can return (recover) to the ground state by radiationless transfer to another molecule such as the ED,[22]

$$^1Dye^* + ED \rightarrow Dye + ED. \tag{4}$$

It can also revert or recover back to the ground state, Dye, by the emission of a photon by a process called fluorescence[22]

$$^1Dye^* \rightarrow Dye + h\nu. \tag{5}$$

The singlet excited state can also undergo intersystem crossing into the more stable and longer-lived triplet state $^3Dye$ (see flow chart in Fig. 1)[18,20]

$$^1Dye^* \rightarrow {}^3Dye^*. \tag{6}$$

This triplet state dye molecule can return (recover) to ground state by radiationless transfer or by delayed emission of a photon. At high dye concentrations the triplet state dye molecules can also be deactivated by collision with another dye molecule

$$^3Dye^* + Dye \rightarrow 2Dye. \tag{7}$$

The dye molecules can also undergo a reaction whereby it abstracts two hydrogen molecules, for example from the ED to form the transparent or clear (leuco) form of the dye.[13,18,20,23]

The actual production of primary radicals ($ED^\bullet$ or $R^\bullet$) takes place when the triplet state dye reacts with the ED. The ED donates an electron to the excited triplet state of the dye leaving the dye with one unpaired electron and an overall negative charge

$$^3Dye^* + ED \rightarrow Dye^{\bullet-} + ED^{\bullet+}. \tag{8}$$

The ED radical cation then loses a proton and becomes a free radical

$$ED^{\bullet+} \rightarrow ED^\bullet + H^+, \tag{9}$$

where the free radical, $ED^\bullet$, is equivalent to the primary radical, $R^\bullet$, appearing in Eqs. (1) and (2).

When a monomer molecule, $M$, is present the primary radical can undergo two possible reactions. The first of these reactions is the initiation of the monomer radical species, $M_1^\bullet$, shown in Eq. (2), and the second involves the radical undergoing dye bleaching.[13,18,20,23] This occurs when the dye radical formed in Eq. (8) abstracts a hydrogen molecule from the ED free radical, as shown in Eqs. (10a) and (10b). This results in the production of an unstable ED intermediate, $[(HOCH_2CH_2)_2NCH{=}CHOH]$, and the transparent dihydro form of the dye, $H_2Dye$,

$$ED^\bullet + H^+ + Dye^{\bullet-} \rightarrow (HOCH_2CH_2)_2NCH = CHOH + H_2Dye, \tag{10a}$$

or equivalently

$$R^\bullet + H^+ + Dye^{\bullet-} \rightarrow R + H_2Dye. \tag{10b}$$

The unstable intermediate then rearranges to form a more stable form. Dye bleaching is an important process because it allows a grating to be fixed after recording. By bleaching any remaining dye, no new free radicals can be formed by exposure. This results in the grating layer becoming transparent.

It has also been reported[15,20,24–26] that the primary radicals produced in Eq. (9) can be scavenged by reacting with inhibitor molecules such as any initially dissolved oxygen (see $Z$ in the flow chart in Fig. 1). This reaction can be described as

$$ED^\bullet + Z \xrightarrow{k_z} (ED + Z^\bullet \text{ and/or } EDZ^\bullet), \tag{11a}$$

or equivalently

$$R^\bullet + Z \xrightarrow{k_z} (R + Z^\bullet \text{ and/or } RZ^\bullet), \tag{11b}$$

where $Z$ is the inhibitor concentration and $k_z$ is the inhibition rate constant. All of these processes, i.e., Equations (1), (11a), and (11b), are summarized in Fig. 1.

### B. Primary radical generation

The flow chart in Fig. 1 presents the main photochemical mechanisms involved in the generation of primary radicals during photoillumination. The rate-determining step for the production of these primary radicals is

$$R_i = 2\Phi I_a(t), \tag{12}$$

where $R_i$ is the rate of generation of primary radicals, $I_a(t)$ (Einstein/cm$^3$ s) is the time varying absorbed intensity, and $\Phi$ is the number of primary radicals initiated per photon absorbed. The factor of 2 again indicates that radicals are created in pairs. The time varying absorbed intensity in Eq. (12) can be expressed using an adaptation of the Beer–Lambert law[15]

$$I_a(t) = I_0'\{1 - \exp[-\varepsilon A(t)d]\}/d, \tag{13}$$

where $I_0'$ (Einstein/cm$^2$ s) is the incident intensity corrected for Fresnel and scattering losses, $\varepsilon$ (cm$^2$/mol) is the molar-absorption coefficient, and $d$ (cm) is the photopolymer layer thickness.

The time varying photosensitizer concentration, $A(t)$ (equivalent to Dye in the Sec. II A) can be expressed using the general rate equation[23,27]

$$\frac{dA(t)}{dt} = -\phi I_a(t) + k_r[A_0 - A_b(t) - A(t)], \tag{14}$$

where $\phi$ (mol/Einstein) is the quantum yield for the elimination of the photosensitizer, and $A_0$(mol/cm$^3$) is the initial photosensitizer concentration. We note that the quantum yield, $\phi$, is not equal to the number of primary radicals initiated per photon absorbed, $\Phi$.

The second term on the right hand side of Eq. (14) (Ref. 27) describes the regeneration or recovery of photosensitizer molecules back to their active ground state, where they are available for further photon absorption, see Fig. 1. The rate constant for this reaction is $k_r$(s$^{-1}$) and $A_b(t)$ represents the concentration of photosensitizer that is bleached, or brought to its clear nonabsorptive state (leuco or $H_2$Dye) during exposure, see Fig. 1. The first term on the right hand side of Eq. (14),[23] which signifies the removal of the photosensitizer, occurs at a much faster rate than the regeneration rate and therefore dominates the photosensitizer processes during short exposures.

As the generation of primary radicals (which is the driving function of the polymerization of monomer) is dependent on the amount of light absorbed by the photosensitizer, it is necessary to examine the temporal evolution of absorption both during and postexposure. In the Sec. III, two limiting cases of Eq. (14) are examined and experiments are proposed and carried out in order to determine the parameters and rates, which dictate the photosensitizer behavior.

## III. TEMPORAL EVOLUTION OF PHOTOSENSITIZER CONCENTRATION

The work carried out in this section is split up into three subsections. The first (Sec. III A), which provides the basis of the other subsections, contains the theoretical analysis of the two limiting cases of the rate equation presented in Eq. (14). These two limiting cases are (a) during exposure and (b) postexposure. The second, Sec. III B, describes the experimental examination of the temporal evolution of the photosensitizer concentration during exposure, i.e., the first limiting case. The third, Sec. III C, examines the effects of photosensitizer recovery and photobleaching postexposure.

### A. Limiting regimes of photosensitizer concentration

Examining the rate equation in Eq. (14) we see that there are two limiting cases, (a) during exposure, $0 < t < t_{\text{exp}}$, and (b) postexposure, $t \geq t_{\text{exp}}$, where $t_{\text{exp}}$ represents the exposure time.

#### 1. During exposure ($0 < t < t_{exp}$)

It is assumed in this analysis that the rate of removal or destruction of the photosensitizer in Eq. (14) is much faster than the regeneration or recovery rate. This assumption is verified experimentally later in the paper. Therefore, during exposure, the rate of removal of photosensitizer dominates the rate equation in Eq. (14) allowing us to write that[23]

$$\frac{dA(t)}{dt} = -\phi I_a(t). \tag{15}$$

Substituting the expression for the absorbed intensity $I_a(t)$ shown in Eq. (13) gives

$$\frac{dA(t)}{dt} = -\frac{\phi}{d} I_0'\{1 - \exp[-\varepsilon A(t)d]\}. \tag{16}$$

Integrating both sides with respect to time yields an expression for the time varying photosensitizer concentration, $A(t)$ (mol/cm$^3$ s), and is given by

$$A(t < t_{\text{exp}}) = (\varepsilon d)^{-1} \ \ln\{1 + [\exp(\varepsilon d A_0) - 1]\exp(-\varepsilon\phi I_0' t)\}. \tag{17}$$

Substituting this solution for the photosensitizer concentration, $A(t)$, back into Eq. (13), yields the time evolution of the absorbed intensity, which can be expressed as

$$I_a(t) = \frac{I_0'[\exp(\varepsilon d A_0) - 1]\exp(-\varepsilon\phi I_0' t)}{1 + [\exp(\varepsilon d A_0 - 1)]\exp(-\varepsilon\phi I_0' t)}. \tag{18}$$

When the exposure intensity is incident on the photopolymer material, the light is either absorbed, $I_a(t)$, transmitted, $I_T(t)$, or lost. This can be represented by

$$I_0' = I_0 T_{\text{sf}} = I_a(t) + I_T(t), \tag{19}$$

where $T_{\text{sf}}$ is a loss fraction that takes into account Fresnel and scattering losses. A normalized transmittance function can also be defined, $T(t) = I_T(t)/I_0$, where $I_0$ (Einstein/cm$^2$ s) is the incident intensity before Fresnel correction. Combining these results gives that

$$T(t) = \frac{I_0' - I_a(t)}{I_0},$$

$$= \frac{T_{sf} I_0'}{I_0'} \left\{ 1 - \frac{[\exp(\varepsilon d A_o) - 1]\exp(-\varepsilon \phi I_0' t)}{1 + [\exp(\varepsilon d A_o - 1)]\exp(-\varepsilon \phi I_0' t)} \right\},$$

$$= \frac{T_{sf}}{1 + [\exp(\varepsilon d A_0) - 1]\exp(-\varepsilon \phi I_0' t)}. \quad (20)$$

This essentially follows the result of Carretero *et al.*[23]

#### 2. Postexposure ($t \geq t_{exp}$)

The second limiting case of Eq. (14) is when $t \geq t_{exp}$. This corresponds to the processes, which occur after the incident light is switched off, and hence when no new photons are available to be absorbed by the photopolymer material, i.e., $I_a(t)=0$. Postexposure photosensitizer effects become important when theoretically modeling or predicting the storage capabilities of a multiply exposed photopolymer. If holographic exposure (or storage) is discontinued for an extended period of time, it is necessary to know the quantity of photosensitizer that will be available for absorption and production of radicals during later recordings.

In this case the rate equation derived from Eq. (14) after the light has been switched off is

$$\frac{dA(t)}{dt} = k_r [A_0 - A_b(t_{exp}) - A(t)]. \quad (21)$$

Integrating both sides of Eq. (21) enables an analytical expression for the time varying recovery or regeneration of photosensitizer for $t \geq t_{exp}$. This analytical expression is given as

$$A(t) = [A_0 - A_b(t_{exp})] - [A_0 - A_b(t_{exp}) - A(t_{exp})] \times \exp[-k_r(t - t_{exp})], \quad (22)$$

where $A(t_{exp})$ and $A_b(t_{exp})$ represent the concentrations of photosensitizer and bleached photosensitizer, respectively, at time $t_{exp}$.

In this subsection, analysis of the two limiting cases of the rate equation, which predicts the concentration of photosensitizer with time, have been presented. Two approximate analytic expressions for the concentration of photosensitizer in these limiting cases have been developed. These mechanisms include photosensitizer recovery and bleaching. In Secs. III B and III C, we examine the experimental behavior and using Eqs. (20) and (22) estimate key physical parameters.

### B. Photon absorption

Based on the photoinitiation mechanisms presented in Sec. II and the processes of photon absorption present during photoillumination described in Sec. III A 1, it can be seen that three main parameters are predicted to determine the absorptive effects of a photopolymer material. These parameters are (i) the quantum yield for the destruction of the photosensitizer, $\phi$, (ii) the molar-absorption coefficient, $\varepsilon$, and (iii) the loss fraction, $T_{sf}$. We now extract values for these important parameters, which control the temporal evolution of absorption effects and, as a result, the photopolymerization mechanisms of grating formation. We do this by fitting experimentally obtained transmittance curves using Eq. (20).

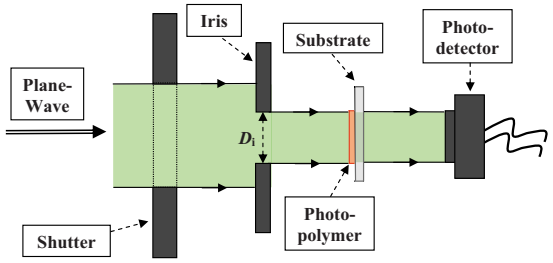


FIG. 2. (Color online) Experimental setup used to monitor time varying transmittance curves.

To obtain estimates for these absorption parameters, we measured the time varying transmittance for a normally incident plane wave of wavelength $\lambda = 532$ nm, see Fig. 2. In order to remove any possible effects due to the diffusion of photosensitizer from outside the exposed regions, the illumination beam exposed the entire photopolymer material layer. The photopolymer material was prepared in the same manner as presented in Refs. 18 and 20. The photosensitizer used was Erythrosin B, which is sensitive at a wavelength $\lambda = 532$ nm. The initial concentration used was $A_0 = 1.22 \times 10^{-6}$ mol/cm$^3$.

As shown in Fig. 2, the illuminating plane wave, which is controlled using a mechanical shutter, propagates through an iris of diameter, $D_i$. The measured intensity, $I_0$, is then incident on the photopolymer material layer. The amount of light transmitted through the material during exposure is monitored using a photodetector. As the photodetector measures intensity in mW/cm$^2$, it is necessary to convert these measurements into Einstein/cm$^2$ s, for use in the expression presented in Sec III A. This is done using

$$I_0' = I_0 \left( \frac{\lambda}{N_a h c} \right) T_{sf}, \quad (23)$$

where $\lambda$ (nm) is the wavelength of incident light, $N_a$ (mol$^{-1}$) is Avogadro's constant, $c$ (m/s) is the speed of light, and $h$ (J s) is Plank's constant. The monitored transmission curves are then normalized with respect to the incident intensity, $I_0'$ (corrected for scattering losses using $T_{sf}$) and then fit using a nonlinear fitting algorithm and Eq. (20). In this way estimates for $\varepsilon$, $\phi$, and $T_{sf}$ are obtained. Figure 3(a) shows a typical experimental transmission curve (dots) with nonlinear fit (solid line) for an exposure of $I_0' = 4$ mW/cm$^2$ and a material layer thickness of $d = 100$ $\mu$m. Figure 3(b) shows the time varying photosensitizer concentration, $A(t)$, generated from the results presented in Fig. 3(a) using Eq. (17).

In order to obtain accurate estimations of the absorption parameters $\varepsilon$, $\phi$, and $T_{sf}$, a set of experiments were carried out. First, several transmission curves were measured for an exposure intensity of 5 mW/cm$^2$ incident on a set of standard material layers, each with different layer thicknesses, $d(\mu m)$. The resulting parameter values produced by nonlinear fits to this experimental data are presented in Table I. As

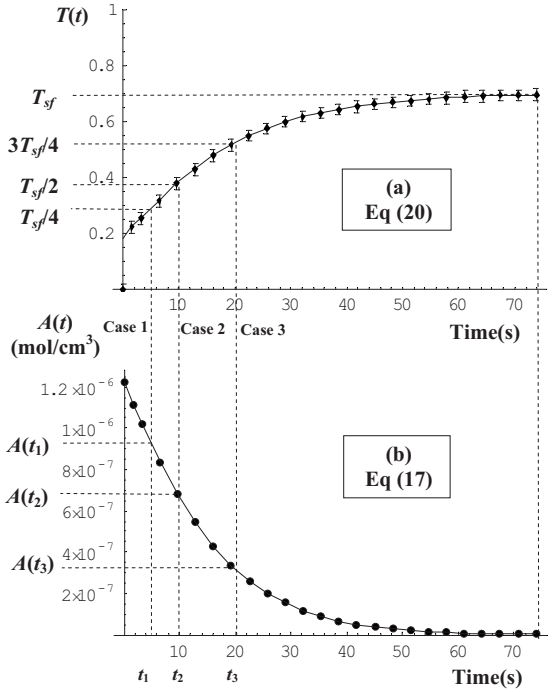


FIG. 3. (a) Experimental data and nonlinear fit to a transmission curve, $T(t)$, using Eq. (20) with error bars indicating experimental reproducibility, and (b) the corresponding photosensitizer concentration, $A(t)$.

can be seen from Table I the parameters estimated for the different material layer thicknesses are similar, and a mean value for each of the absorption parameters is presented. These values are of the same order as those obtained by Carretero *et al.*[23] using the same methods. Second, several transmission curves were measured for a range of exposure intensities, all of which were incident on a standard material layer of thickness $d=120$ $\mu$m. The absorption parameters were again estimated and are presented in Table II. Once again there is a good general agreement between each of the estimated parameters, and those attained by Carretero *et al.*,[23] and the mean values obtained in both tables do not differ significantly. Further verification of the absorption parameters obtained are presented in Refs. 28 and 29.

For the transmittance curve presented in Fig. 3(a), cases, 1, 2, and 3 correspond to exposure times, $t_1$, $t_2$, and $t_3$, respectively, which result in a particular fraction of light transmitted through the photopolymer. These fractions correspond to one-quarter, $T_{sf}/4$, one-half, $T_{sf}/2$, and three-quarters, $3T_{sf}/4$ of the maximum intensity that is transmitted at saturation, $T_{sf}$, i.e., the maximum amount of light that can be

TABLE I. Parameter values extracted from fits to experimental transmittance curves for a range of material layer thicknesses. In all cases $I_0'=5$ mW/cm$^2$.

| Thickness ($\mu$m) | $\varepsilon$ (cm$^2$/mol) ($\times10^8$) | $\phi$ (mole/Einstein) | $T_{sf}$ |
|---|---|---|---|
| 80 | 1.333 | 0.0356 | 0.792 |
| 120 | 1.437 | 0.0370 | 0.800 |
| 160 | 1.549 | 0.0350 | 0.780 |
| Mean | $1.440\pm0.109$ | $0.036\pm0.001$ | $0.7375\pm0.0625$ |

TABLE II. Parameter values estimated from transmittance curves for a range of intensities and constant layer thickness $d=120$ $\mu$m.

| Intensity (mW/cm$^2$) | $\varepsilon$ (cm$^2$/mol) ($\times10^8$) | $\phi$ (mole/Einstein) | $T_{sf}$ |
|---|---|---|---|
| 2 | 1.416 | 0.0390 | 0.792 |
| 4 | 1.452 | 0.0326 | 0.800 |
| 6 | 1.450 | 0.0330 | 0.780 |
| Mean | $1.390\pm0.127$ | $0.035\pm0.004$ | $0.7375\pm0.0625$ |

transmitted after taking into account the Fresnel and scattering losses. $A(t_1)$, $A(t_2)$, and $A(t_3)$ are then the photosensitizer concentrations at these particular exposure times. This description now forms the basis of the methods used to measure the concentrations of photosensitizer regenerated and bleached as discussed in SecIII C.

## C. Postexposure measurements

Using the analysis presented in Sec. III A 2, we now examine the effects of regeneration and bleaching of the photosensitizer.

### 1. Recovery process

As discussed in Sec. II, when a photopolymer material is illuminated with an appropriate light intensity, the photosensitive dye molecules absorb photons and are excited to the singlet, $^1$Dye, and/or triplet, $^3$Dye, state forms of the photosensitizer. As can be seen from the flow chart in Fig. 1, these excited states can result in the production of free radicals, ED$^\bullet$, or can be converted to the leuco or dihydro states, $H_2$Dye, or can return to the unexcited ground state, Dye, which is available for the reabsorption of photons.

The analysis carried out in this section attempts to estimate the rate, $k_r$, at which the photosensitizer recovers or returns back to its initial ground state form. In order to achieve this, a set of experiments is performed, which enables the photosensitizer concentration to be approximated at any time, $t$, after a given exposure time, i.e., $t_{exp}$.

By exposing standard material layers of thickness, $d=100$ $\mu$m, to an incident intensity, $I_0'=4$ mW/cm$^2$, the transmittance curves were monitored in the same manner as that described in Sec. III B. From these data, the exposure times necessary to reach one-quarter, one–half, and three-

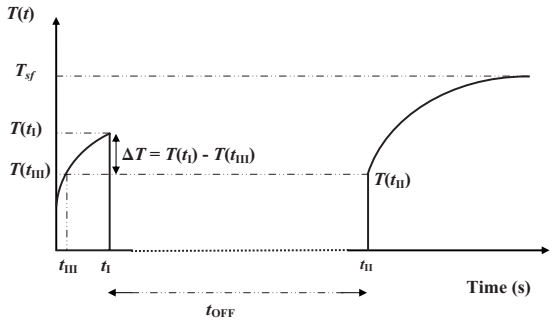


FIG. 4. Schematic of the experimental processes involved to determine the rate of recovery of photosensitizer after an exposure, $t_I$.

quarters of the saturated value of transmittance, $T_{sf}$, see Fig. 3(a), were identified. These times are denoted by $t_1$, $t_2$, and $t_3$ respectively. From this information, the experiment to determine the rate of recovery can be carried out using the following five steps: (see Fig. 4)

(1) Expose a standard material layer of uniform thickness, $d$, for time $t_I$, i.e., the exposure time required to obtain one quarter of the saturated value of transmittance, i.e., $T_{sf}/4$.
(2) Turn off the exposing light using the mechanical shutter for a period of time $t_{off}$.
(3) Open the shutter after the time $t_{off}$ (when $t=t_{II}$) and record the transmitted intensity.
(4) Calculate the difference in the transmitted intensity, $\Delta T$, between the light transmitted at time $t_I$, i.e., $T(t_I)$, and time $t_{II}$, i.e., $T(t_{II})$, and convert these differences in transmittance into the corresponding photosensitizer concentrations, i.e., $A(t_I)$ and $A(t_{II})$.
(5) Repeat for different values of $t_{off}$ in order to quantify the time evolution of these changes in transmittance and thus photosensitizer concentration.

Figure 4 is a schematic representation of the experimentally observed transmittance behavior used to determine the rate of recovery of the photosensitizer. This schematic representation is used because the recovery of the photosensitizer is a much slower process than the instantaneous transmittance. Thus the time axis in the schematic is chosen to make the experimentally observed effects more clearly visible.

In order to approximate the concentration of the photosensitizer at the required times, i.e., $t_I$ and $t_{II}$, it is necessary to relate Eqs. (17) and (20), as was done in Fig. 3. This means that the transmittance at any time, $T(t)$, corresponds to a photosensitizer concentration at that time, $A(t)$. Also, it is assumed that the photosensitizer concentration corresponding to the light transmitted at time $t_{II}$, i.e., $A(t_{II})$ in Fig. 4, is the same concentration that corresponds to an equal transmittance at time, $t_{III}$, i.e., $A(t_{III})$ in Fig. 4. This then allows us to use Eq. (17) to predict the photosensitizer concentration for the light transmitted for any value of $t_{off}$. We can therefore write that

$$A(t_{II}) = A(t_{III}), \quad \text{since} \quad T(t_{II}) = T(t_{III}). \tag{24}$$

By determining from the experimental data, the difference in the amount of light transmitted, $\Delta T$, from the time when the light was switched off, $T(t_I)$, to the time the light was switched back on, $T(t_{II})=T(t_{III})$, the amount of photosensitizer recovered, $A_r$, during the postexposure period $t_{off}$ can be calculated,

$$A_r(t_{off}) = A(t_{III}) - A(t_I). \tag{25}$$

This process is repeated for varying values of $t_{off}$ so that a full description of the photosensitizer recovery process can be obtained. At small values of recovery time, $t_{off}$, the amount of the recovered photosensitizer will be small. This value will get progressively larger for larger recovery times (see Fig. 5) until the amount of photosensitizer available to recover is reduced (due to bleaching). This behavior is described using Eq. (22).

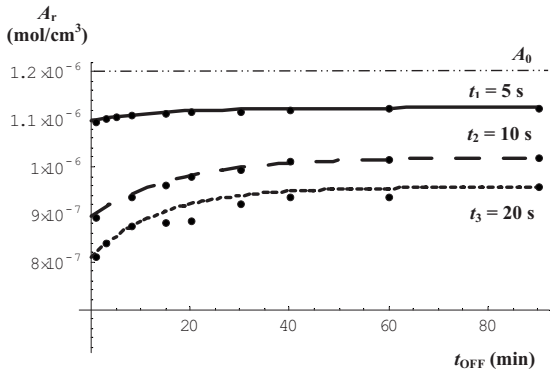


FIG. 5. Theoretical fit to experimentally determined photosensitizer recovery concentration for three different exposure times: $t_1=5$ s (solid line), $t_2=10$ s (long dashed line), and $t_3=20$ s (short dashed line).

To find the rate at which the photosensitizer recovers, $k_r(s^{-1})$, in our photopolymer material, three different exposure times were examined, i.e., $t_1=5$ s, $t_2=10$ s, and $t_3=20$ s. For each of these cases, experimental transmittance curves were obtained for a range of values of $t_{off}$. From these transmittance curves, the concentration of photosensitizer recovered was calculated using Eq. (17). The experimental results are presented in Fig. 5 for each of the three different exposure times. These times correspond to one-quarter, one-half, and three-quarters of the $T_{sf}$, as shown in Fig. 3.

The three photosensitizer recovery curves were then fit using Eq. (22), which predicts the temporal evolution of photosensitizer recovery, postexposure. The theoretical fits are shown as lines in Fig. 5.

The value of $A(t_{exp})$, which represents the concentration of photosensitizer when the light has been switched off, is extracted from the experimental data and is presented in Table III. The value of the bleached photosensitizer concentration, $A_b$, which will be discussed in Sec. III C 2, is assumed to be the amount of photosensitizer, which did not recover by $t_{off}=90$ min, i.e., $A_b(t_{exp})=A_0-A_r$ ($t_{off}=90$ min), where $A_0$ is the initial photosensitizer concentration. Fitting the experimental data, the rate constant of recovery of the photosensitizer, $k_r$, is then estimated. The values obtained are presented in Table III.

As can be seen, the rate constant of recovery, $k_r$, is almost the same for each of the three cases examined. This is not surprising since the possible effects of photosensitizer diffusion from outside the exposed regions have been removed, i.e., the total layer area is exposed. However, even if this was not the case, it is unlikely that photosensitizer diffusion would have much of an effect, as the Erythrosin B molecular weight is 879.92 g/mol, making it relatively large

TABLE III. Extracted parameter values from fits to experimental determined photosensitizer recovery curves.

| $t_{exp}$ (s) | $T(t)$ | $A(t_{exp})$ (mol/cm$^3$) ($\times 10^{-6}$) | $A_b(t_{exp})$ (mol/cm$^3$) ($\times 10^{-7}$) | $k_r$ ($s^{-1}$) ($\times 10^{-3}$) |
|---|---|---|---|---|
| $t_1=5$ | $T_{sf}/4$ | 1.096 | 2.130 | 1.19 |
| $t_2=10$ | $T_{sf}/2$ | 0.894 | 6.798 | 1.22 |
| $t_3=20$ | $3T_{sf}/4$ | 0.810 | 9.632 | 1.17 |

and immobile in the cross-linked acrylamide/polyvinylalcohol (AA/PVA) photopolymer system.

Also, the values obtained for the rate constant of recovery shown in Table III are significantly slower than the rate at which the photosensitizer is removed (of the order of minutes). Thus verifying the assumption made in Sec. III A 1 that during exposure the effects of recovery can be assumed negligible.

The results presented here indicate that there is a significant amount of photosensitizer recovery over extended periods of time in this material. Since for larger initial exposures more dye molecules become excited, therefore, up to a certain exposure time, more photosensitizer will be available for recovery or regeneration. This process is obviously significant for data storage applications in photopolymers that are similar to the AA/PVA, photopolymer material studied here.

### 2. Bleaching process

The bleached form of the photosensitizer (leuco and $H_2Dye$) is produced when a dye radical, $Dye^{\bullet -}$, see Eq. (8), abstracts a hydrogen molecule from the ED free radical, $ED^{\bullet}$, i.e., $R^{\bullet}$, as shown in Eqs. (10a) and (10b). The rate equation for this process can be given by

$$\frac{dA_b(t)}{dt} = k_b\left[\frac{A(t)R^{\bullet}(t)}{\beta}\right], \tag{26}$$

where $k_b$ is the rate constant of photobleaching of the photosensitizer and $\beta$ indicates the fraction of photosensitizer and primary radicals, which react to form the inert form of the photosensitizer. In order to solve Eq. (26) and estimate physical values for $k_b$ and $\beta$, the corresponding set of coupled differential equations should be derived and solved. However, in this section, a simple phenomenological model to predict the time varying photosensitizer concentration and extract estimations of the photobleaching rate constant, $k_b$, is presented.

First a set of experiments was carried out with the aim of calculating the concentration of photosensitizer bleached during exposure. This was done using the setup presented in Fig. 2. In these experiments, the transmitted light was monitored for varying exposure times, spanning the entire duration of the transmittance curve, i.e., Fig. 3(a). In all cases a constant exposure intensity, $I_0'=4$ mW/cm$^2$, was normally incident on standard material layers of thickness $d=100$ $\mu$m.

The exposure time, $t_{\text{exp}}$, was varied and following exposure value $t_{\text{off}}=12$ h ($\sim\infty$) was chosen. This large value of $t_{\text{off}}$ allows all recovery processes (for each particular length of exposure) to completely take place. When the incident light is switched back on, the amount of light transmitted is recorded and the difference, $\Delta T$, between this value and the transmittance value $T(t_{\text{exp}})$ is determined. Using Eq. (17), the corresponding concentrations of photosensitizer can be calculated enabling the concentration bleached, $A_b(t_{\text{exp}})$, to be estimated.

Figure 6 shows a schematic representation of the photosensitizer processes, which occur during and postexposure. The decaying curve illustrates the temporal behavior of the photosensitizer concentration, $A(t)$, when the material is continuously exposed. The three increasing exponential curves show the behavior of the recovery of the photosensitizer for exposures $t_1$ (solid line), $t_2$ (long dashed line), and $t_3$ (short dashed line). The corresponding quantities bleached for each exposure are denoted as $A_b(t_1\rightarrow\infty)$, $A_b(t_2\rightarrow\infty)$, and $A_b(t_3\rightarrow\infty)$.

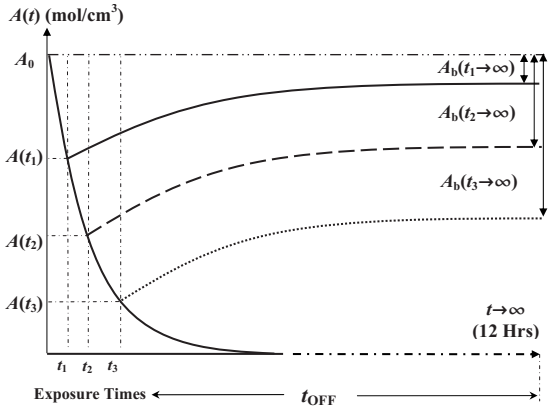


FIG. 6. Schematic representation of the experiments carried to calculate the concentration of photosensitizer bleached per second of exposure.

The experimental data obtained from this process are presented in Fig. 7. As can be observed, with increased exposure time, the concentration of bleached photosensitizer, $A_b(t)$, increases slowly. This process continues until all the photosensitizer has been bleached.

The experimental data presented in Fig. 7, for the concentration of photosensitizer bleached per second of exposure, were fit using the simple expression

$$A_b(t) = A_0[1 - \exp(-k_b I_0' t)], \tag{27}$$

where $A_0$ is the initial photosensitizer concentration and $I_0'$ is the exposure intensity, which is corrected for Fresnel and scattering losses. $k_b=6.18\times10^5$ cm$^2$/Einstein is the rate constant extracted from the best fit to the data in Fig. 7. Table IV shows the values obtained for $A_b(t)$ by fitting the experimental results in the three cases presented in Secs. III B and III C 1 for $t_1=5$ s, $t_2=10$ s, and $t_3=20$ s.

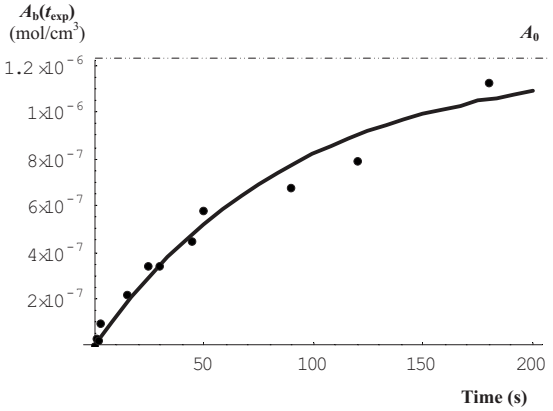


FIG. 7. Concentration of bleached photosensitizer (dots) obtained experimentally as a function of exposure time and a best fit using Eq. (27) (solid line).

TABLE IV. Experimental results obtained for $t_{off}=12$ h ($\sim\infty$).

| $t_{exp}$ (s) | $T(t)$ | $A(t_{exp})$ (mol/cm$^3$) ($\times 10^{-6}$) | $A_b(t_{exp})$ (mol/cm$^3$) ($\times 10^{-7}$) |
|---|---|---|---|
| $t_1=5$ | $T_{sf}/4$ | 1.080 | 0.697 |
| $t_2=10$ | $T_{sf}/2$ | 0.788 | 1.350 |
| $t_3=20$ | $3T_{sf}/4$ | 0.629 | 2.560 |

As can be observed in Fig. 7, a reasonably good fit is achieved to the experimental data using the simple phenomenological model proposed, i.e., Eq. (27). However, we note that the values for the concentration of bleached photosensitizer presented in Table IV differ with those presented in Table III. There are three plausible reasons for this: (i) the assumption made in Sec. III C 1, for determining the rate constant of recovery that after $t_{off}=90$ min, the difference between the concentration $A(t_{off}=90$ min) and the initial photosensitizer concentration, $A_0$, was the concentration of bleached photosensitizer, $A_b(t)$; (ii) the use of a simple function to model the rate of change of photosensitizer, i.e., Eq. (27) (a more complete model is clearly necessary to accurately predict this behavior); and/or (iii) the data presented in Fig. 7 show the concentration of photosensitizer bleached for an exposure time which is greater than that required to reach the saturated transmittance, $T_{sf}$, i.e., $t_{exp}>t_{Tsf}$. However, the experimental data set presented does not illustrate the full range of photosensitizer bleaching behavior. The data tend to suggest that due to the effects of recovery and regeneration, a significantly longer exposure time is necessary to fully bleach all the photosensitizer.

## IV. DISCUSSION AND CONCLUSIONS

Starting with a detailed description of the photoinitiation mechanisms taking place in the AA/PVA based photopolymer material, we have further developed a rate equation to include the effects of both the recovery and the bleaching processes, which arise during photon absorption in photopolymer materials. Quantitatively understanding these effects increases our ability to predict the time evolution of grating formation during and postexposure.

It was previously shown that the main process responsible for consuming photosensitizer concentration was photosensitizer absorption. In this paper, an expression for the change in the absorbed intensity during exposure is presented and the key material parameters controlling the absorption characteristics are estimated. Experiments have been carried out to find the rate constants of the recovery and bleaching processes using postexposure experimental data. The results obtained tend to agree for a large range of experimental parameter values. Further work is required to more accurately describe these effects, including longer exposure times, larger ranges of intensities, and a more complete theoretical model describing the effects of photosensitizer bleaching. However, the work presented here clearly shows that the postexposure photosensitizer effects taking place in such photopolymer materials can make a significant enough contribution to require their inclusion in any comprehensive material model.

## ACKNOWLEDGMENTS

We acknowledge the support of the Enterprise Ireland and Science Foundation Ireland through the Research Innovation and Proof of Concept Funds and the Basic Research and Research Frontiers Programs. We would also like to thank the Irish Research Council for Science, Engineering and Technology and SPIE through the SPIE Educational Scholarship.

[1] L. Dhar, A. Hale, H. E. Katz, M. L. Schilling, M. G. Schnoes, and F. C. Schilling, Opt. Lett. **24**, 487 (1999).
[2] L. Dhar, A. Hale, K. Kurtis, M. G. Schnoes, M. Tackitt, W. Wilson, A. Hill, M. Schilling, H. Katz, and A. Olsen, *Conference Digest, Optical Data Storage* (IEEE, New York, 2000), pp. 158–160.
[3] S. Schultz, E. Glytsis, and T. Gaylord, Appl. Opt. **39**, 1223 (2000).
[4] A. Sato, M. Scepanovic, and R. Kostuk, Appl. Opt. **42**, 778 (2003).
[5] J. T. Sheridan, J. V. Kelly, G. O'Brien, M. R. Gleeson, and F. T. O'Neill, J. Opt. A, Pure Appl. Opt. **6**, 1089 (2004).
[6] R. R. McLeod, A. J. Daiber, M. E. McDonald, T. L. Robertson, T. Slagle, S. L. Sochava, and L. Hesselink, Appl. Opt. **44**, 3197 (2005).
[7] T. D. Milster, Opt. Photonics News **16**, 28 (2005).
[8] J. T. Sheridan, J. V. Kelly, M. R. Gleeson, C. E. Close, and F. T. O'Neill, J. Opt. A, Pure Appl. Opt. **8**, 236 (2006).
[9] Aprilis, HMC Media, 2006, www.aprilisinc.com/datastorage_media.htm
[10] InPhase Technologies, Tapestry Media, 2007, www.inphase-technologies.com
[11] C. Carre, D. J. Lougnot, and J. P. Fouassier, Macromolecules **22**, 791 (1989).
[12] C. Carre and D. J. Lougnot, J. Opt. (Paris) **21**, 147 (1990).
[13] S. Blaya, L. Carretero, R. F. Madrigal, M. Ulibarrena, P. Acebal, and A. Fimia, Appl. Phys. B: Lasers Opt. **77**, 639 (2003).
[14] S. Gallego, M. Ortuno, C. Neipp, A. Marquez, A. Belendez, I. Pascual, J. V. Kelly, and J. T. Sheridan, Opt. Express **13**, 1939 (2005).
[15] G. Odian, *Principles of Polymerization* (Wiley, New York, 1991).
[16] A. Zakrzewski and D. C. Neckers, Tetrahedron **43**, 4507 (1987).
[17] G. Manivannan, P. Leclere, S. Semal, R. Changkakoti, Y. Renotte, Y. Lion, and R. A. Lessard, Appl. Phys. B: Lasers Opt. **58**, 73 (1994).
[18] J. R. Lawrence, F. T. O'Neill, and J. T. Sheridan, Optik (Stuttgart) **112**, 449 (2001).
[19] M. D. Goodner and C. N. Bowman, Macromolecules **32**, 6552 (1999).
[20] M. R. Gleeson, J. V. Kelly, D. Sabol, C. E. Close, S. Liu, and J. T. Sheridan, J. Appl. Phys. **102**, 023108 (2007).
[21] J. B. Birk, *Organic Molecular Photophysics* (Wiley, New York, 1975), Vol. 2.
[22] A. Gilbert and J. Baggott, *Essentials of Molecular Photochemistry* (Blackwell Scientific, Oxford, 1991).
[23] L. Carretero, S. Blaya, R. Mallavia, R. F. Madrigal, A. Belendez, and A. Fimia, Appl. Opt. **37**, 4496 (1998).
[24] A. Fimia, N. Lopez, F. Mateos, R. Sastre, J. Pineda, and F. Amatguerri, J. Mod. Opt. **40**, 699 (1993).
[25] A. K. O'Brien and C. N. Bowman, Macromol. Theory Simul. **15**, 176 (2006).
[26] A. V. Galstyan, S. Hakobyan, S. Harbour, and T. Galstian, http://e-lc.org/Documents/T.__V_Galstian_2004_05_05_11_13_17.pdf
[27] M. R. Gleeson, D. Sabol, S. Liu, C. E. Close, J. V. Kelly, and J. T. Sheridan, J. Opt. Soc. Am. B **25**, 396 (2008).
[28] G. Qiaoxia, H. Mingju, and G. Fuxi, Dyes Pigm. **69**, 204 (2006).
[29] R. G. Stomphorst, G. van der Zwan, M. A. M. J. van Zandvoort, A. B. Sieval, H. Zuilhof, F. J. Vergeldt, and T. J. Schaafsma, J. Phys. Chem. A **105**, 4235 (2001).